High-Gain Wideband SIW-Fed Tri-Pentagonal Prism Dome for 6G Application

Sidhartha Kumar Sahu, Rakhesh Singh Kshetrimayum, and Ramesh Kumar Sonkar

Abstract – This paper introduces a high-gain slotted substrate integrated waveguide-fed stacked tri-pentagonal prism dome dielectric resonator antenna. The use of a unique parasitic patch design inside the slot of a substrate-integrated waveguide (SIW) helps to achieve high gain in the SIW structure. Owing to the pentagonal prism stacking structure, the novel dielectric resonator antenna (DRA) design offers high gain and a wide bandwidth. The antenna prototype is designed, fabricated, and measured. The antenna offers a 1.43-GHz (8.52–9.95 GHz) bandwidth, along with a peak gain of 11.5 dBi. The antenna exhibits a broadside radiation pattern. The difference between copolarization and cross-polarization is more than 21 dB in both the E-plane and H-plane. The front-to-back ratio is 34.33 dB. The half-power beamwidth (HPBW) is 29°. The stacked DRA is lightweight compared with ceramic DRAs due to the three-dimensional printing method. The antenna operates in the 5G new radio frequency range 3 band. This antenna is suitable for 6G applications.

1. Introduction

With the rapid growth of wireless communication, user density has increased significantly, as has reliance on multiple devices such as personal computers, tablets, and smartphones. Emerging applications, such as virtual reality-based holographic teleportation and industrial automation, demand ultra-low latency and extremely high data rates, surpassing the capabilities of 5G. In Addition, increasing network density also requires improved energy efficiency, which remains a challenge for 5G [1]. Conventional cellular networks, where each base station serves a defined set of user equipment, have long been standard. However, they suffer from inter-cell interference, particularly for users at cell edges [2]. Cell-free massive multiple-input multiple-output (CF-mMIMO) addresses this by employing multiple distributed access points to jointly serve users, reducing interference and path loss while enhancing spectral efficiency and macro-diversity [3]. The antenna proposed in this work is well-suited for deployment in access points within CF-mMIMO architectures. CF-mMIMO can achieve high-capacity, low-latency, and high-reliability requirements of next-generation 6G applications. In 6G, the intercell interference can be non-existent, and spatial diversity will be increased using CF-mMIMO architecture [4].

Frequency range 3 (FR3) is receiving much of attention because of its high data rates. This is because the spectrum needs to be expanded beyond frequency range 1 (FR1) and frequency range 2 (FR2). This band addresses key challenges in indoor signal propagation, where traditional frequencies experience Ricean fading, and mmWave suffers from severe body losses. Unlike FR1, which is crowded, and FR2, which has high path loss and fading, FR3 strikes a good balance by offering an empty spectrum, lower path loss, and better propagation. This makes it the best choice for future wireless communication systems [5]. The range of the FR3 band is 7 GHz to 24 GHz. The antenna presented here works within the FR3 band.

The antenna contains both a substrate-integrated waveguide (SIW) and a dielectric resonator antenna (DRA). SIWs offer low loss, high-quality factors, and improved power handling compared with microstrip antennas [6]. DRAs offer thermal stability, design flexibility, and strong polarization discrimination, thereby enhancing signal quality [7]. Their integration enables wideband, high-gain, broadside radiation and scalability to mmWave and sub-THz bands, critical for cell-free networks. Unlike conventional microstrip or patch antennas, the DRA radiating structure is composed entirely of dielectric material, eliminating conductive paths within the radiating region. This characteristic minimizes conductor and surface wave losses, which become more prominent at higher frequencies. This single antenna can also be made a MIMO antenna by adding a few more elements. Owing to SIW and DRA, the port isolation and gain will be high in the MIMO antenna.

High-gain antennas are vital in wireless communication systems, as they enhance signal integrity, coverage, and efficiency. By directing transmitted power, they extend coverage while minimizing attenuation and interference. Their ability to improve signal-to-noise ratio enables higher data rates and enhances network reliability and performance. Antenna arrays are commonly employed to attain high gain; however, their design is often intricate and bulky, resulting in elevated power consumption. Additionally, mutual coupling among array elements deteriorates performance [8]. As an alternative

Manuscript received 7 March 2025. The dielectric constant measurement is supported by the iHUB Divyasampark Technology Innovation Hub (TIH), IIT Roorkee (Project TIH/RP/05). This work is supported by the Science and Engineering Research Board, India, under Grant CRG/2023/000316.

Department of Electronics and Electrical Engineering, IIT Guwahati, Guwahati, India.

Sidhartha Kumar Sahu, Rakhesh Singh Kshetrimayum, and Ramesh Kumar Sonkar are with the Indian Institute of Technology Guwahati, Assam, 781039, India; e-mail: ksidhartha@iitg.ac.in, krs@iitg.ac.in, sonkar@iitg.ac.in.

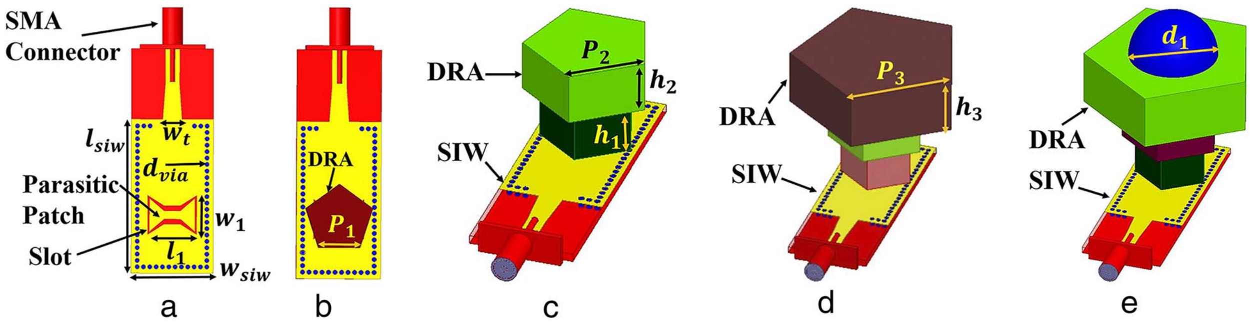

Figure 1. Antenna structure development. (a) S-1: Geometry of SIW antenna without any DRA (dimensions in mm: $l_{siw} = 12$, $w_{siw} = 12$, $l_1 = 12$, $w_1 = 9.5$, $w_t = 4.7$, $d_{via} = 1.1$, $h_{cyl} = 8$). (b) S-2: Geometry of pentagonal prism DRA placed on SIW. (c) S-3: Geometry of 2-layer pentagonal prism DRA placed on SIW, (d) S-4: Geometry of 3-layer pentagonal prism DRA. (e) S-5: Geometry of stacked pentagonal prism dome DRA (dimensions in mm: $p_1 = 11$, $p_2 = 14.67$, $p_3 = 25.73$, $h_1 = 10$, $h_2 = 10$, $h_3 = 13.9$).

approach, stacked DRAs offer a more efficient solution for achieving high gain while mitigating these limitations [9]. In the antenna presented here, three pentagonal prism and hemispherical DRAs are stacked on one another to enhance the gain.

A DRA with a flipped, stair-shaped configuration consisting of three pentagonal prism-shaped dielectric resonators has been developed for wideband applications. This structure supports multiple resonant modes, enabling wideband operation through closely spaced broadside modes. An air gap between the DRA layer and the SIW enhances impedance matching and radiation efficiency. The design meets wideband requirements for 6G, offering high-speed, low-interference, and multiband performance.

Traditional DRA stacking using adhesives can disrupt permittivity, impedance matching, and structural accuracy under stress. Three-dimensional–printed DRAs eliminate glue and air gaps, enhancing precision, stability, and electromagnetic performance for high-frequency applications [10]. This antenna is significantly lighter than traditional ceramic DRAs.

In [11], a stair-shaped structure is used to achieve wideband performance. However, the antenna's gain is relatively low. In the present structure, the gain of the antenna is almost double the gain in [11]. In [12], a stair-shaped DRA is used to achieve a dual band operation in the sub-6-GHz band. However, the gain of the antenna is less (i.e., 6 dBi). In [13], a stacked triangular-shaped DRA is used to achieve ultrawideband performance. However, the gain of the antenna is very low. In [14], SIW-fed stacked DRA exhibits narrowband along with a peak gain of 9.62 dBi. In [15], the antenna is designed for CF-mMIMO applications and features a narrowband in the FR1 band, with a gain of approximately 8.4 dBi. In [16], the antenna attains 18 dBi gain using a 16-element antenna array, whereas the proposed antenna achieves 11.5 dBi with a single element. Unlike antenna arrays, the proposed stacked DRA design avoids inter-element coupling issues and size constraints, thereby offering a high-gain and wideband solution suitable for space-limited and high-frequency applications. In the present work, a combination of SIW and the stacked tri-pentagonal prism dome DRA offers a wideband response along with high gain, making it suitable for access points in 6G applications. This shape of DRA has not been reported previously in any literature.

2. Antenna Design

The stagewise antenna design development is shown in Figure 1. Figure 2 (a), (b), (c), and (d) present the comparative results of bandwidth, gain, electric field (E-field), and magnetic field (H-field), respectively, for the designed prototype at various stages of development. The dimensions of the antenna are: $l_{siw} = 12$ mm, $w_{siw} = 12$ mm, $l_1 = 12$ mm, $w_1 = 9.5$ mm, $w_t = 4.7$ mm,

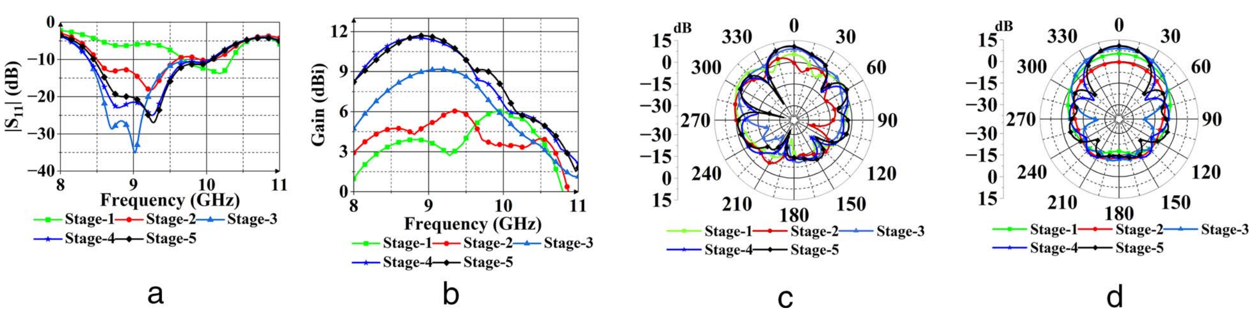

Figure 2. Comparison between different stages as follows: (a) $|S_{11}|$ vs frequency plot, (b) gain vs frequency plot, (c) E-plane radiation pattern, and (d) H-plane radiation pattern.

Table 1. Comparison between different stages of SIW-fed DRA

Stage No.	Bandwidth (GHz)	Peak Gain (dBi)
Stage 1	9.72–10.33 (6.08%)	5.96
Stage 2	8.51–9.60 (12.03%)	6.05
Stage 3	8.40–10.02 (17.58%)	9.17
Stage 4	8.40–10.00 (17.4%)	11.5
Stage 5	8.45–10.08 (17.6%)	11.7

$d_{via} = 1.1$ mm, $h_{cyl} = 8$ mm, $p_1 = 11$ mm, $p_2 = 14.67$ mm, $p_3 = 25.73$ mm, $h_1 = 10$ mm, $h_2 = 10$ mm, $h_3 = 13.9$ mm. In stage 1 (S-1), a triangular dumbbell-shaped slot is etched on the SIW surface. The SIW consists of a substrate, an upper metal layer, and a ground plane. In this antenna, FR4 substrate is used, whose relative dielectric permittivity (ϵ_r) is 4.4 and loss tangent ($\tan\delta$) is 0.02. The substrate thickness is 1.6 mm. The dimensions of SIW are decided using the equations given in [17]. A triangular dumbbell-shaped parasitic patch is placed inside the slot (Figure 1a). The purpose of placing a parasitic patch is to achieve a higher gain. The bandwidth and gain obtained in S-1 is 610 MHz (9.72–10.33 GHz) and 5.96 dBi. The bandwidth and gain for each stage are shown in Table 1. In stage 2 (S-2), a pentagonal DRA is placed on the slotted SIW (Figure 1b). The DRA is fabricated using a three-dimensional printing process. The material used for DRA is polyactic acid (PLA). The bandwidth and gain in S-2 are 1.09 GHz (8.51–9.60 GHz) and 6.05 dBi. The bandwidth increases by 480 MHz due to the pentagon structure.

In stage 3 (S-3), a stacked pentagon is placed on SIW (Figure 1c). The structure exhibits a bandwidth of 1.62 GHz (8.40–10.02 GHz) and a peak gain of 9.17 dBi. The bandwidth increases by 530 MHz. The air gap between the second layer of DRA and SIW is the reason behind the bandwidth enhancement. The gain also increases by 3.12 dBi. In stage 4 (S-4), a three-layer stacked pentagon is placed on a slotted SIW (Figure 1d). The bandwidth remains almost the same, but the gain increases by 2.33 dBi. In stage 5 (S-5), a tri-pentagonal prism dome DRA is placed on a slotted SIW. The addition of a hemispherical DRA increases the bandwidth, gain, and beam width. The final structure offers a bandwidth of 1.63 GHz (8.45–10.08 GHz) and a peak gain of 11.7 dBi.

3. Results and Discussion

The comparison between simulation and measurement results is shown in Figure 3a. The measured bandwidth is slightly less than the simulated bandwidth due to the fabrication tolerance. The bandwidth measurement is done using a vector network analyzer. The measurement setup is shown in Figure 3b. The dielectric constant of PLA is also measured using the vector network analyzer and dielectric assessment kit software. The test setup is shown in Figure 3c. The DRA is fabricated using PLA material ($\epsilon_r = 2.45$, $\tan\delta = 0.004$). The dielectric constant and loss tangent plot are shown in Figure 4d. The PLA material can withstand temperatures up to 170°C and exhibit a tensile strength of 52 MPa at yield [18].

The gain and radiation pattern measurement is done inside the anechoic chamber. The anechoic chamber setup is shown in Figure 4a. The measured gain obtained is 11.5 dBi. High gain is achieved by exciting the DRA in higher-order mode. The radiation pattern in both the E-plane and H-plane is shown in Figure 4. The difference between copol and cross-pol in the E-plane and H-plane is more than 21 dB in the broadside direction. Owing to the high difference between copol and cross-pol, the interference in the signal is less. The front-to-back ratio is 34.33 dB, and the HPBW is 29°. Wider beamwidth is achieved from hemispherical DRA. Wider-beamwidth antennas can offer more coverage. The antenna is linearly polarized. Because of the three-dimensional printing method, this antenna is lightweight compared with traditional DRAs. The antenna weighs around 47 g. The antenna performance is compared with existing literature in Table 2. The parasitic patch and stacked DRA configuration enable the achievement of broadside bandwidth and high gain compared with other antennas operating in the 5G new radio FR3.

4. Conclusion

This work presents a novel SIW design that incorporates a parasitic patch within its slot, significantly enhancing gain and bandwidth compared with conventional narrowband SIW structures. In addition, to get even better radiation performance, a stacked tri-pentagonal

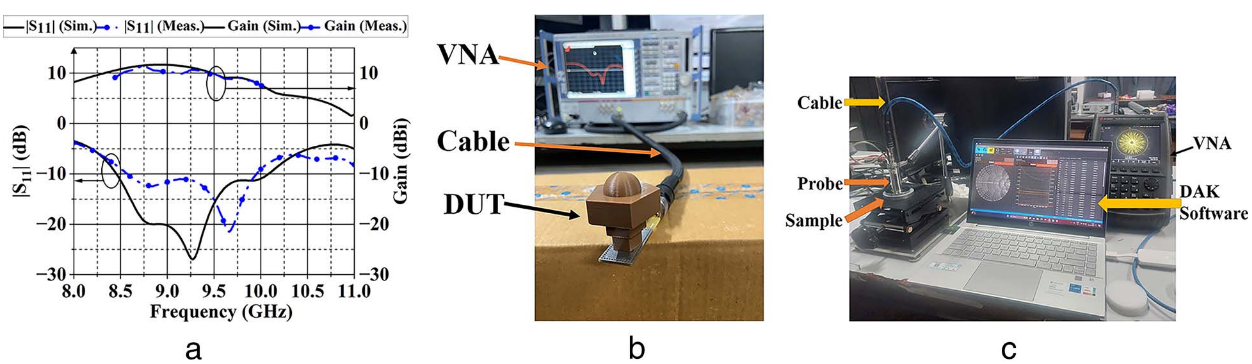

Figure 3. (a) Comparison between simulation and measurement results of $|S_{11}|$ and gain vs frequency plot. (b) Measurement of $|S_{11}|$ vs frequency plot using Vector Network Analyzer (VNA). (c) Material dielectric constant measurement setup using VNA.

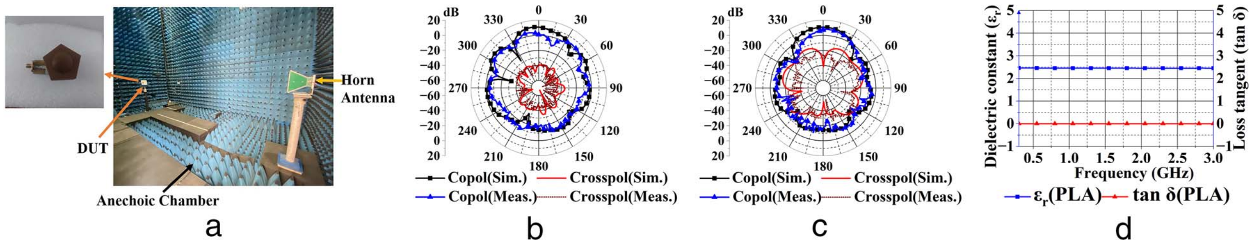

Figure 4. (a) Gain and radiation pattern measurement setup in the anechoic chamber. (b) Simulated and measured copolar and cross-polar radiation patterns in the E-plane. (c) Simulated and measured copolar and cross-polar radiation patterns in the H-plane. (d) Dielectric constant and loss tangent vs frequency plot.

Table 2. Comparison between other 5G antennas available for 5G NR FR3 band

Ref.	Antenna technology	Bandwidth (GHz)	Peak Gain (dBi)	Fabricated?
[19]	SIW Antenna	11.12–11.84 (6.27%)	10.4	No
[20]	SIW antenna	10.42–10.98 (5.23%)	10.82	Yes
[21]	Slot antenna	8.5–9.9 (15.2%)	5.8	Yes
[22]	Slot antenna	9.47–9.72 (2.6%)	8.9	No
[23]	SIW antenna	10.2–11.62 (2.35%)	9.22	Yes
This work	SIW-fed stacked DRA	8.52–9.95 (15.48%)	11.5	Yes

prism dome-shaped DRA is attached to the slotted SIW. This combined structure effectively optimizes both gain and operational bandwidth. This antenna exhibits 15.48% (8.52–9.95 GHz) bandwidth, along with a peak gain of 11.5 dBi. The difference between copol and cross-pol is good because of the presence of DRAs. The front-to-back ratio is 34.33 dB. The HPBW is 29°. The antenna is linearly polarized. This antenna is suitable for access points in the cell-free networks proposed for 6G applications.

5. References

1. I. F. Akyildiz, A. Kak, and S. Nie, “6G and Beyond: The Future of Wireless Communications Systems,” *IEEE Access*, **8**, 2020, pp. 133995-134030.
2. M. Karakayali, G. Foschini, and R. Valenzuela, “Network Coordination for Spectrally Efficient Communications in Cellular Systems,” *IEEE Wireless Communications*, **13**, 4, 2006 pp. 56-61.
3. S. Buzzi and C. D’Andrea, “Cell-Free Massive Mimo: User-Centric Approach,” *IEEE Wireless Communications Letters*, **6**, 6, 2017, pp. 706-709.
4. W. Jiang, B. Han, M. A. Habibi, and H. D. Schotten, “The Road Towards 6G: A Comprehensive Survey,” *IEEE Open Journal of the Communications Society*, **2**, 2021, pp. 334-366.
5. D. Shakya, M. Ying, T. S. Rappaport, H. Poddar, P. Ma, et al., “Comprehensive fr1(c) and fr3 Lower and Upper Mid-Band Propagation and Material Penetration Loss Measurements and Channel Models in Indoor Environment for 5G and 6G,” *IEEE Open Journal of the Communications Society*, **5**, 2024, pp. 5192-5218.
6. M. Bozzi, L. Perregrini, K. Wu, and P. Arcioni, “Current and Future Research Trends in Substrate Integrated Waveguide Technology,” *Radioengineering*, **18**, 6, 2009.
7. A. Petosa and A. Ittipiboon, “Dielectric Resonator Antennas: A Historical Review and the Current State of the Art,” *IEEE Antennas and Propagation Magazine*, **52**, 5, 2010, pp. 91-116.
8. S. Fakhte, I. Aryanian, and L. Matekovits, “Analysis and Experiment of Equilateral Triangular Uniaxial-Anisotropic Dielectric Resonator Antennas,” *IEEE Access*, **6**, 2018, pp. 63071-63079.
9. A. A. Kishk, “Directive Yagi–Uda Dielectric Resonator Antennas,” *Microwave and Optical Technology Letters*, **44**, 5, 2005 pp. 451-453.
10. C. Sarkar, D. Guha, and C. Kumar, “Glueless Compound Ground Technique for Dielectric Resonator Antenna and Arrays,” *IEEE Antennas and Wireless Propagation Letters*, **16**, 2017, pp. 2440-2443.
11. R. Chair, A. Kishk, K. Lee, and C. Smith, “Broadband Aperture Coupled Flipped Staired Pyramid and Conical Dielectric Resonator Antennas,” IEEE Antennas and Propagation Society Symposium, 2004, Monterey, California, June 20–25, 2004, pp. 1375-1378.
12. M. Zou and J. Pan, “Wide Dual-Band Circularly Polarized Stacked Rectangular Dielectric Resonator Antenna,” *IEEE Antennas and Wireless Propagation Letters*, **15**, 2016, pp. 1140-1143.
13. Z. Song, H. Zheng, M. Wang, Y. Li, T. Song, et al., “Equilateral Triangular Dielectric Resonator and Metal Patch Hybrid Antenna for UWB Application,” *IEEE Access*, **7**, 2019, pp. 119060-119068.
14. S. K. Sahu, R. S. Kshetrimayum, and R. K. Sonkar, “High Gain and Dual Band SIW-Fed Stacked Conical DRA for 5G NR FR1 Application,” presented in the 2024 18th European Conference on Antennas and Propagation (EuCAP), Glasgow, UK, March 17–22, 2024.
15. S. K. Sahu, R. S. Kshetrimayum, R. K. Sonkar, and A. Kumar, “High Gain SIW-Fed Notched Spherical-Frustum Shaped Stacked DRA for B5G Application,” presented in the 2025 19th European Conference on Antennas and Propagation (EuCAP), Stockholm, Sweden, March 30–April 4, 2025.
16. H. Yang, J. Lu, C. Lin, C. Song, and G. Gao, “Design of wideband cavity-backed slot antenna with multilayer

dielectric cover," *IEEE Antennas and Wireless Propagation Letters*, **15**, 2016, pp. 861-864.

17. F. Xu and K. Wu, "Guided-Wave and Leakage Characteristics of Substrate Integrated Waveguide," *IEEE Transactions on Microwave Theory and Techniques*, **53**, 1, 2005, pp. 66-73.
18. A. Haleem, V. Kumar, and L. Kumar, "Mathematical Modelling and Pressure Drop Analysis of Fused Deposition Modelling Feed Wire," *International Journal of Engineering and Technology*, **9**, 4, 2017, pp. 2885-2894.
19. G. J. Paliwal, A. Kumar, and J. Sengupta, "SIW Cavity-Backed Slot Antenna Using High-Order Radiation Modes for Broadband Applications in X Band," presented in the 2023 IEEE International Symposium on Antennas and Propagation (ISAP), Kuala Lumpur, Malaysia, October 30–November 2, 2023.
20. A. Kumar Nayak, I. M. Filanovsky, K. Moez, and A. Patnaik, "A Low Profile Improved Gain SIW-Based H-Plane Horn Antenna for X-Band Application," 2023 IEEE International Symposium on Antennas and Propagation and USNC-URSI Radio Science Meeting (USNC-URSI), Portland, Oregon, July 23–28, 2023, pp. 1647-1648.
21. S. Biswas, A. Kumar, S. Chowdhury, V. K. Singh, and S. Chakrabarti, "A Circularly Polarized Cavity-Backed Conformal Antenna With Wide Sectoral Coverage and Low Cross Polarization for High Power X-Band Airborne Application," presented in the 2023 IEEE Microwaves, Antennas, and Propagation Conference (MAPCON), Ahmedabad, India, December 11–14, 2023.
22. E. V. Goud, Y. M. Kumar, R. R. Reddy, and A. V. Lakshmi, "A Moon Shaped Slotted Pentagonal Patch Antenna With DGS for High-Gain and X Band Applications," presented in the 2024 IEEE Wireless Antenna and Microwave Symposium (WAMS), Visakhapatnam, India, February 29–March 3, 2024.
23. G. J. Paliwal, A. Kumar, and J. Sengupta, "Bandwidth Enhancement of SIW Cavity Backed Slot Antenna Using High-Order Radiation Modes," presented in the 2024 IEEE Wireless Antenna and Microwave Symposium (WAMS), Visakhapatnam, India, February 29–March 3, 2024.